Beyond the Hybridization Effects in Plasmonic Nanoclusters: Diffraction-Induced Enhanced Absorption and Scattering

Mohsen Rahmani, Andrey E. Miroshnichenko, Dang Yuan Lei, Boris Luk' yanchuk, Michael I. Tribelsky, Arseniy I. Kuznetsov, Yuri S. Kivshar, Yan Francescato, Vincenzo Giannini, Minghui Hong, and Stefan A. Maier**

It is demonstrated hererin both theoretically and experimentally that Young's interference can be observed in plasmonic structures when two or three nanoparticles with separation on the order of the wavelength are illuminated simultaneously by a plane wave. This effect leads to the formation of intermediate-field hybridized modes with a character distinct of those mediated by near-field and/or far-field radiative effects. The physical mechanism for the enhancement of absorption and scattering of light due to plasmonic Young's interference is revealed, which we explain through a redistribution of the Poynting vector field and the formation of near-field subwavelength optical vortices.

1. Introduction

More than two hundred years ago, Thomas Young[1] demonstrated that light from two or three coherent sources of a double or triple slit is accompanied by remarkable interference effects, and this observation laid the foundation to the modern wave theory of light. Young's interference effects usually take place between coherent sources at distances of the order of the wavelength. Plasmonic nanoparticles illuminated by a plane wave can also realize such a system of coherent sources, which hence could demonstrate similar interference phenomena. Indeed, electromagnetic near-field

Dr. M. Rahmani[+]
Data Storage Institute, A*STAR (Agency for Science Technology and Research), DSI Building, 5 Engineering Drive 1, 117608, Singapore
Dr. M. Rahmani
Department of Physics
Imperial College London, London, SW7 2AZ, United Kingdom
Dr. M. Rahmani
Department of Electrical and Computer Engineering
National University of Singapore, 117576, Singapore
Dr. A. E. Miroshnichenko,[+] Prof. Y. S. Kivshar
Nonlinear Physics Centre
Research School of Physics and Engineering
Australian National University
Canberra, ACT 0200, Australia
Dr. D. Y. Lei[+]
Department of Applied Physics
The Hong Kong Polytechnic University
Hong Kong, China
Prof. B. S. Luk'yanchuk, Dr. A. I. Kuznetsov
Data Storage Institute
A*STAR (Agency for Science Technology and Research), DSI Building, 5 Engineering Drive 1, 117608, Singapore
Prof. M. I. Tribelsky
Faculty of Physics
M. V. Lomonosov Moscow State University
Moscow 119991, Russia; Technical University MIREA
119454, Moscow, Russia
Y. Francescato, Dr. V. Giannini, Prof. S. A. Maier
Department of Physics
Imperial College London, London, SW7 2AZ, UK
E-mail: s.maier@imperial.ac.uk
Prof. M. H. Hong
Department of Electrical and Computer Engineering
National University of Singapore
117576, Singapore
E-mail: elehmh@nus.edu.sg
[+]These authors contributed equally to this work.

DOI: 10.1002/smll.201301419

NANO MICRO small

coupling effects between neighboring plasmonic nanostructures play an important role in nanophotonics, and are useful for applications in sub-diffraction imaging, solar cells, biosensing and medicine. The most remarkable examples include metamaterials with negative refraction indices[2–4] and optical nanoantennas.[5,6] Yet plasmonic interference effect mediated by wavelength-scale interaction, in analogy to Young's experiment, has attracted much less attention.

Coupling effects in periodic nanostructures such as plasmonic gratings,[7–10] nanoparticle chains[11–15] or photonic crystals,[16,17] have been explained by phenomena like diffraction coupling,[18] lattice modes,[14,19,20] Wood's anomaly[21] and the Talbot effect.[22] Such structures may exhibit higher absorption than single elements due to Bragg scattering.[23] The enhanced absorption of light in these structures is particularly important for future data storage technology and photovoltaic cells.[24,25] In spite of many ideas suggested in this field (see e.g., Refs. [24–28]), tailoring the plasmonic response through coherent interactions remains a very active field of interest. On the other hand, coupling effects in systems consisting of a finite number of particles with nanoscale gaps are more complicated, and the field enhancement in such systems was investigated mostly for applications such as surface-enhanced Raman scattering.[12,29] Field enhancement generally dominates at small separation distances between particles, and can be described in terms of plasmon hybridization theory,[30–33] valid for the near-field coupling. At larger separations, hybridization effects disappear and plasmonic nanoparticles arranged in non-periodical fashion are generally supposed as non-interacting.[34,35] Thus, neither hybridization nor Wood's anomaly models can be applied to explain coupling among well-separated isolated particles. In spite of a few research works devoted to fill this gap with explanations based on radiation coupling,[8,11,36–40] an analytical method that can provide a physically intuitive picture of coupling effects in complex nanostructures with wavelength-scale separation is still missing. Moreover, in order to study coupling effects with separation distance, mostly systems composed of similar components such as metallic spheres,[11,37] cylinders,[41] pillars,[18] disks[32,34] or bars[38,42–44] have been used. Since the individual components in the aforementioned systems exhibit similar resonances, coupling effects mainly result in red or blue shifts in the dominant plasmon resonance of an individual unit.

In this paper we study an analogy between Young's experiment and light scattering of plasmonic structures. First, we show that this analogy can be found in a simple complex consisting of two plasmonic nanoparticles with variable separation distance (see **Figure 1**a). Since both nanoparticles are illuminated by the same plane wave, this system is expected to show a direct similarity to Young's interference experiment, in which a coherent beam passes through double slits to obtain wave interference. We analyze light scattering by these two nanoparticles employing a dipole approximation with effective polarizabilities. Since the total field acting on a particular particle consists of contributions from the excitation field and the field induced by the other particle, a dyadic Greens function can be used to calculate the total scattered field of the entire dimer, therefore modeling the whole complex as two interacting dipoles. The corresponding consideration reveals periodic appearances of extinction and absorption maxima at $D = n\lambda$, where D is the interparticle distance and λ is the resonance wavelength. This theoretical observation is further verified in experiment by measuring the extinction intensity of Au dimers as a function of distance. Though this finding is not entirely surprising, it allows to obtain a unified picture of coupling among nanostructures from nanoscale interparticle gap to separations of the order of the resonant wavelength.

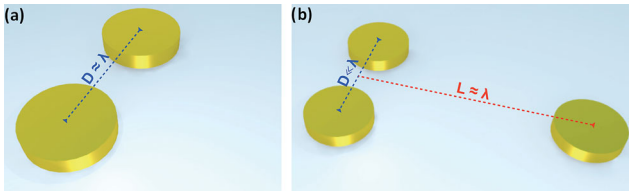

Figure 1. Illustration of complexes of a) an isolated plasmonic dimer and b) a trimer composed of a dimer plus monomer (DpM).

Most importantly, we show that when two inhomogeneous elements such as an isolated dimer and a monomer (see Figure 1b) get close to distances of $L = n\lambda$, the coupling between their respective electromagnetic fields results in a formation of a new resonant mode that can be associated with a "Young resonance". Theoretical analysis of the Poynting vector distribution in such a system consisting of three nanoparticles reveals a signature of optical vortices. This is in a close analogy to Young's experiment[1] with triple slits, in which the wave intensity vanishes at the point of singular phase,[45,46] leading to a circulation of electromagnetic energy. We show that for certain wavelengths and interparticle distances, Young's interference in plasmonic systems dominates over all other plasmonic modes, and that such vortices result in a remarkable enhancement of both scattering and absorption. This observation can be attributed to variations in field-lines of the vector Poynting field.

2. Plasmonic Dimers

First, we study the extinction response of the Au dimer of 145 nm diameter and 60 nm thickness, with a center-to-center distance varying from 160 to 850 nm. The measured and simulated extinction spectra for these dimer systems are shown in **Figures 2**a,b, with Figure 2a for the excitation polarization parallel to the interparticle axis and Figure 2b for the perpendicular polarization, respectively. The black curve in both the figures is a reference spectrum corresponding to the extinction of a single monomer, which exhibits a localized surface plasmon resonance (LSPR) at 660 nm. We can appreciate from Figure 2a that, for two well-separated monomers (distances larger than 850 nm), there is no remarkable variation in the spectral profile with respect to a single monomer. For smaller separations (distances less than 250 nm), the LSPR of the dimer exhibits a significant red shift. Such resonance shift can be well explained by plasmon hybridization theory that predicts a significant decrease of the redshift value with an increase in the interparticle separation.

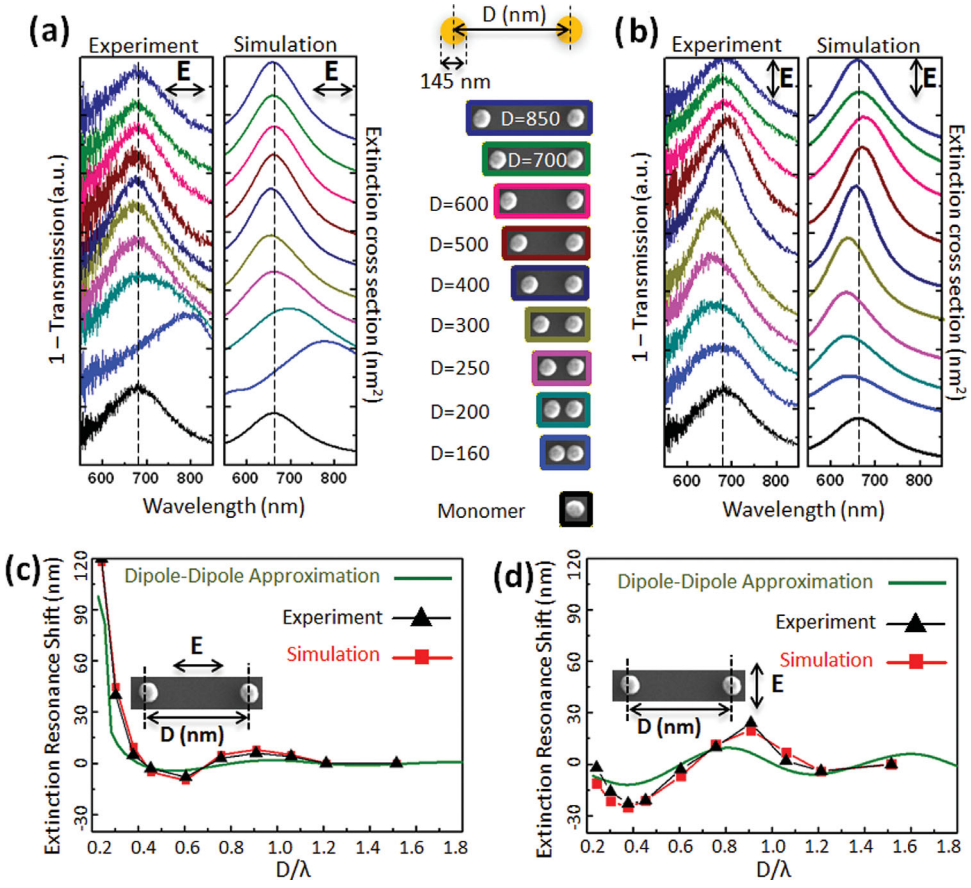

Figure 2. Extinction spectra of dimers with different interparticle separation distances *D* for polarizations a) parallel and b) perpendicular to the interparticle axis. Corresponding SEM images are shown in the middle panel. Diameter and thickness of each single nanodisk is 145 nm and 60 nm, respectively. Vertical dashed lines designate the resonant wavelength λ for the single nanodisk. Simulated (red), experimentally measured (black) and dipole-dipole approximation (green) extinction resonance shift for dimers *vs* ratio of the interparticle distance over the resonance wavelength for c) parallel and d) perpendicular polarizations with respect to the interparticle axis. Experimental and simulated data in c) and d) are extracted from 10 different dimer pairs.

However, numerical results also demonstrate a small blue shift in the separation range from 250 to 500 nm (see Figure 2a). This is a weak effect and has been neglected in the hybridization theory. We will discuss this issue later on. Also note that for the excitation polarization perpendicular to the interparticle axis we observe an opposite situation, where the extinction peak significantly blue-shifts when the separation distance increases from 200 to 400 nm and then red-shifts for the further increase of the distance to ≈500–600 nm. By comparing the different behaviors observed for the two orthogonal polarizations, we can reach at the following qualitative conclusions. The near-field interaction in the dimers is stronger at smaller separations for incident polarization along the axis connecting two monomers, which is in agreement with the theoretical prediction by the plasmon hybridization. Meanwhile, far-field coupling effects at larger separations for the same polarization are very weak due to parallel orientation of the dipole radiative fields from each monomer. The situation completely reverses for the polarization perpendicular to the separation axis: we observe a weak near-field interaction attributed to a parallel alignment of the two induced dipole moments, but relatively a strong far-field interaction enabled by the large overlap of their radiative fields.

Here we show that it is possible to unify the physical description of the complicated separation dependence of field coupling in plasmonic dimers within the framework of the dipole-dipole approximation, which is a standard example of the application of multiple scattering theory.[47,48] By modeling two monomers as two interacting dipoles and treating their radiative scattering[46,49] as the coherent light sources, we have determined the absorption and scattering properties of plasmonic dimers versus separation distance in analogy to Young's experiment.[1] In our calculations, each dimer consists of two plasmonic nanoparticles with radii R_1 and R_2 ($R_{1,2} \ll \lambda$), and separated by a distance $D = |r_2 - r_1|$ where $r_{1,2}$ are the coordinates of the centers of the particles. The effective polarizabilities can be presented as

$$p_{1,2} = \alpha E_{1,2}^{total}, \quad (1)$$

where $p_{1,2}$ are the effective electric dipole moments, $E_{1,2}^{total}$ are the total electric fields acting on the corresponding particle (i.e. the sum of the incident light field and the one

NANO MICRO small

produced by the other dipole) and α is the effective electric polarizability (assuming particles 1 and 2 are identical). In the framework of the Mie theory this polarizability is as follows

$$\alpha = \varepsilon_0 \frac{6i\pi}{k^3} a_1, \tag{2}$$

with a_1 is the electric dipole amplitudes and k stands for the incident light wavenumber. We consider nonmagnetic particles with $\mu = 1$. The solution based on the dyadic Green functions[49] (see the Supporting Information) yields expressions for the extinction and absorption cross sections $C_{ext,abs}$. For polarization parallel to the interparticle axis one can find:

$$C_{ext}^{X} \propto \mathrm{Im}\left[\frac{\alpha}{1-\alpha\frac{\exp(ikD)}{2\pi\varepsilon_0 D^3}(1-ikD)}\right], \tag{3}$$

$$C_{abs}^{X} = \left|\frac{\alpha}{1-\alpha\frac{\exp(ikD)}{2\pi\varepsilon_0 D^3}(1-ikD)}\right|^2. \tag{4}$$

Similar formulas for light polarization perpendicular to the separation axis can be written as:

$$C_{ext}^{Y} \propto \mathrm{Im}\left[\frac{\alpha}{1-\alpha\frac{\exp(ikD)}{4\pi\varepsilon_0 D^3}(3-3ikd-k^2D^2)}\right], \tag{5}$$

$$C_{abs}^{Y} \propto \left|\frac{\alpha}{1-\alpha\frac{exp(ikD)}{4\pi\varepsilon_0 D^3}(3-3ikd-k^2D^2)}\right|^2. \tag{6}$$

In Equations (3–6) one can see the characteristic oscillating terms presented by *sinc*-like functions $\exp(ikD)$ resulting in an oscillatory dependences for $C_{ext,abs}(D)$.

Figure 2c,d shows the comparison among simulated, experimental and theoretical dipole-dipole approximation results on plasmon resonance shift versus interparticle distance of the dimers, for the polarization parallel and perpendicular to the interparticle axis, respectively. In Figures 2c,d each data point represents the shift of the simulated and measured LSPR wavelength of the dimers with respect to the resonance wavelength of the single monomer, and the interparticle distance is normalized to the LSPR wavelength. It is worth mentioning that our analytical dipole-dipole approximation is based on a treatment of spherical nanoparticles in the absence of a substrate. Keeping in mind that as long as a dipole polarization is a concern, the difference in the shape results only in a change of the constants in the polarizability expression, while the dependence of the polarizability on the problem's parameters essentially remains the same. Thus a particle absorbs or emits radiation as a point-like dipole. This justifies that *Au* nanospheres can be used in analytical calculations (based on the Mie scattering method) to predict the optical responses of *Au* nanodisks[50] (control comparison can be seen in Figure S1). Note that such an assumption leads to a slight shift of the calculated plasmon resonances of dimers with respect to the experimental and simulated ones (see Figure 2c,d). A full consideration of the substrate effect is made in our simulations, which results in good agreement between the simulation and experiment.

It can be seen from Figures 2c that for the polarization parallel to the interparticle axis, a large red-shift in extinction resonance appears for separation distance $D/\lambda < 0.3$, whereas the shift approaches zero for $D/\lambda > 1.6$. This dependence can be well explained by the plasmon hybridization theory as discussed previously. However, the hybridization theory cannot explain the pronounced oscillations of the extinction resonance with the normalized interparticle distance in the range of $0.5 < D/\lambda < 1.5$, observed for both the polarizations (see Figure 2c,d) since they are attributed to the effects analogous to Young's double-slit interference lying beyond the applicability of that theory. The good agreement between the theoretical and experimental results shows clearly that the coupled dipole approximation is capable to produce the whole picture of the coupling behavior for both the polarizations. Though some limited parts of the entire coupling map presented in Figure 2 have been documented in previous publications,[32,37,38,51] in what follows we will show that just employing inhomogeneous systems, such as a complex dimer plus monomer (DpM) may reveal the full nature of this complicated coupling map in a wide range of the separation distances. It is worth noting that a similar approach can also be obtained by a consideration of both electric and magnetic dipoles in low-loss semiconductor dimers.[52]

3. Plasmonic Trimers

Now we consider coupling effects in a more complicated inhomogeneous system composed of a packed, fixed size dimer and a monomer at different values of the dimer-monomer separation distance L, see **Figure 3**. In the complex DpM the distance between the two elements of the dimer is always kept equal to 15 nm, so that the hybridization effect within the dimer is unchanged. On the basis of the previous finding on Young's interference effect, we study the optical response of the entire complex for polarization perpendicular to the separation axis when the interference effect is more pronounced. The results for the parallel polarization are provided in Supplementary Information.

Figure 3a shows the measured and simulated extinction spectra for DpM systems at varying separation distance, accompanied with the extinction spectra for the isolated monomer and the isolated dimer (blue and red curves, respectively) for reference. As it can be seen, in DpM systems with separations less than 300 nm, two distinct resonances attributed to contributions of the dimer (around 790 nm) and monomer (around 660 nm) occur, which is consistent with the scenario of plasmon hybridization between the dimer and monomer. The extinction behavior of the systems with separations larger than 700 nm is also not surprising because the resulting spectra are simply the plain, arithmetical sum of the two reference spectra without any interference. However, at the dimer-monomer separation in the range of ≈400–700 nm, a new behavior in the extinction response of the entire complex emerges, as indicated by the shallow pink

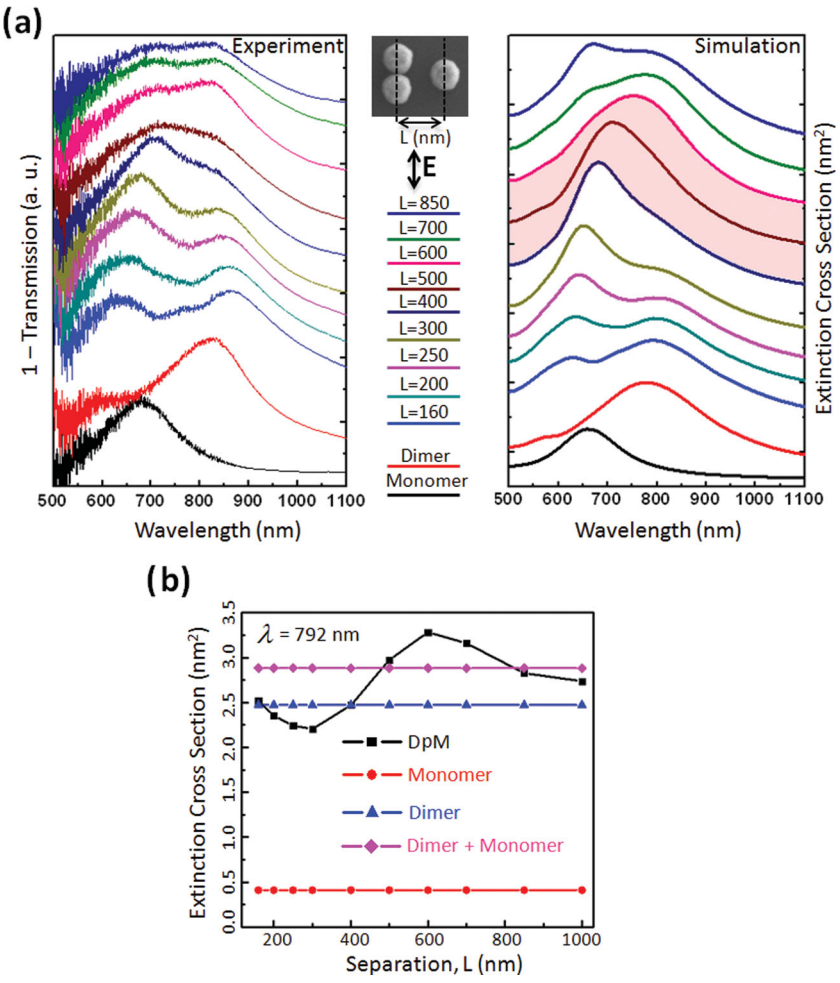

Figure 3. a) Experimentally measured 1-Transmission spectra (left panel) and simulated extinction cross sections (right panel) for DpM at several different separation distances *L* (corresponding to the SEM images in middle panel) for the polarization direction perpendicular to the separation axis. The shadow area in the right panel indicates the separation range where Young's resonance appears. b) The absolute values of the extinction cross section corresponding to indicated structures at the wavelength of 792 nm. Red and blue curves correspond to the isolated monomer and dimer, respectively.

region in Figure 3a, right panel. Specifically, looking at both brown and pink curves corresponding to 500 nm and 600 nm separations, we can identify a new resonance which neither belongs to hybridized modes of the dimer and monomer nor to their separate extinction resonances. This is in agreement with our calculations that show Young's type interference appears for separations on the order of the resonance wavelength. Figure 3b plots the absolute extinction value versus separation distance for the isolated monomer, dimer, their plain arithmetical sum and the DpM complex. An oscillatory behavior of the extinction intensity *vs* separation distance *L* at 792 nm wavelength (the dimer resonant wavelength) for the DpM complex clearly demonstrates the interference effect between the two elements, which may result in the extinction cross section of the combined structure remarkably larger than the plain arithmetical sum of the two non-interacting elements. We have chosen this wavelength for demonstration because of the large extinction intensity from the hybridized dimer resonance; however this oscillatory behavior can be seen at any other wavelength from the specified range of several hundred nanometers.

4. Energy Flow Peculiarities

The most important physical consequences of Young's interference in plasmonic nanostructures are the enhanced scattering and absorption effects that can be better understood in terms of the Poynting vector field, as we will show in what follows. In **Figure 4** we present the contour plots of the scattering (Figure 4b) and absorption (Figure 4c) topography in the separation-wavelength coordinate plane for DpM. We observe that the maximum scattering of the entire system occurs at an optimal separation of 621 nm and the wavelength of 690 nm. The insert in Figure 4b shows the absolute values of scattering cross sections for monomer (curve 1), dimer (curve 2), a plain arithmetical sum of the two (curve 3, no interference effects), and DpM (curve 4, with interference effects), respectively. The difference between curves 3 and 4 reveals the existence of Young's interference that cannot be explained by the hybridization theory because of the large separation distance between the particles. Figure 4d shows the Poynting vector field corresponding to these parameters. As it can be seen from the lower part of the figure, the formation of two optical vortices in front of the dimer effectively blocks the energy flux towards the dimer. The dimer "repels" the Poynting vector lines. It leads to a strong scattering enhancement due to the large bending of Poynting vector lines around the dimer and hence to an overall peak in the extinction cross section of the entire system. This is a direct analogy to Young's experiment where light vanishes at some fringes of interference of the three waves at such locations where the light intensity is zero (the centers of the vortices), and the phase is singular. In general, all 2π phase values occur around the zero intensity points, leading to a circulation of the electromagnetic energy around them.[45,46] These points, known as optical vortex nodes arising from interference between two crossed standing waves,[53,54] have been studied in quantum interference and entanglement in radiating systems.[45] Note here that radiation pressure produced by optical vortices can greatly influence diffusion of metallic nanoparticles.[54]

More interesting effects in the DpM complex may be observed for absorption. As we can see from Figure 4c at L = 365 nm and wavelength 571 nm, the maximal absorption cross section of the entire complex is significantly larger than the plain sum of the ones for the dimer and monomer

NANO MICRO small

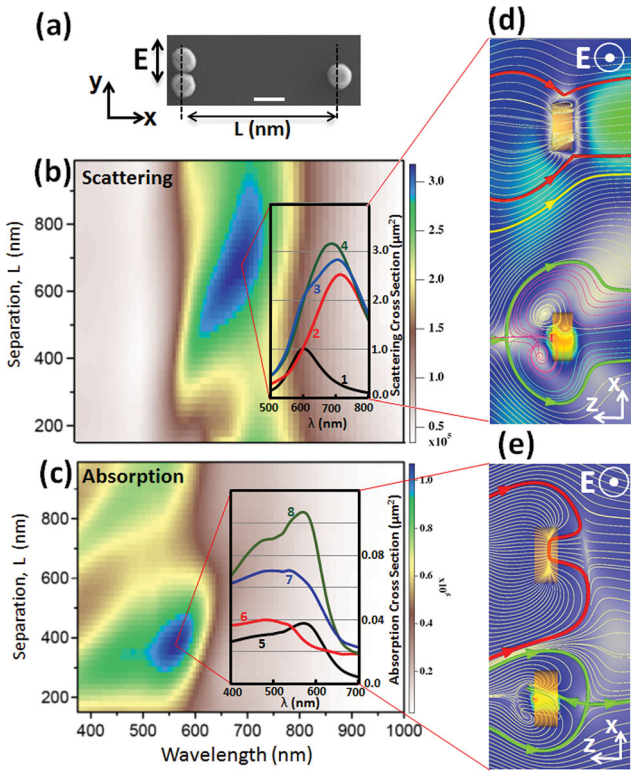

Figure 4. a) SEM image of the DpM structure and the orientation of coordinates and vector E of the incident wave. Scale bar is 200 nm. b) Calculated dependence of the scattering and c) absorption cross sections of DpM as a function of wavelength and dimer-monomer separation distance *L*. d) Poynting vectors at the wavelength of 690 nm and separation of 621 nm corresponding to the scattering maximum, and e) the wavelength of 571 nm and separation of 365 nm corresponding to the absorption maximum. Yellow separatrix indicates the boundary between the basins of attraction of the Poynting vector field-lines for the dimer and monomer, respectively. Red (monomer) and green (dimer) separatrixes designate the basins of attraction for the field-lines, which end in the particles owing to light absorption. Insets in (b) and (c) depict the absolute values of the scattering and absorption cross sections, corresponding to the monomer (curves 1 & 5), dimer (curves 2 & 6), plain arithmetical sum of those for the monomer and dimer (curves 3 & 7) and the entire DpM system (curves 4 & 8), respectively.

taken separately. It raises the natural question – *how can the absorption of a complex be larger than the total absorption of its constituting elements?*

To answer this question, let us consider the Poynting vector field corresponding to the specified values of the separation distance and wavelength, depicted in Figure 4e. The figure reveals the origin of the enhanced absorption, induced by Young's interference. In this case, the absorption cross section of the dimer is close to its geometrical one. However, what the dimer does is an ejection of the electromagnetic field towards the monomer. It enlarges the basin of attraction of the monomer, enhancing the light intensity in the vicinity of the latter, cf. Figures 4d,e. As a result, the absorption cross section of the monomer increases, which in turn increases the overall absorption of the entire complex. This effect can be seen clearly by inspection of the separatrix surfaces (tubes) in the far field.[55,56] All vector lines inside a tube enter the corresponding particle. Thus, the area of a geometrical cross section of a separatrix tube by a plane lying in the far field at $z > 0$ perpendicular to the wave vector of the incident wave (we remind that the incident wave propagates against z-axis) should define the effective absorption cross section of the corresponding components of the DpM (dimer or monomer), while the arithmetical sum of these areas defines the absorption cross section of the entire complex, see **Figure 5**. Note that for a small spherical plasmonic nanoparticle there is the following exact relation between the maximal scattering $\sigma_{sca}^{(max)}$ and absorption $\sigma_{abs}^{(max)}$ cross sections, namely $\sigma_{abs}^{(max)}/\sigma_{sca}^{(max)} = 1/4$.[23,57,58] Importantly, in the case of the enhanced absorption induced by Young's resonance, we can exceed this theoretical limit substantially. This finding provides a unique scenario to understanding the entire coupling mechanism beyond the plasmon hybridization model and may be applied to study more general plasmonic structures. For instance, our finding reveals the importance of coupling among non-neighboring elements in plasmonic aggregated molecules such as plasmonic oligomers.[59] We show that intermediate-field Young-type coupling effects among non-neighboring batches of components within a single oligomer should also be considered (see Supporting Information, Figure S3).

5. Conclusion

To summarize our findings note that in the direct analogy to the classical Young's double-slit interference, we have analyzed the light scattering by two nanoparticles employing a dipole approximation with effective polarizabilities, and revealed the oscillatory behavior of the extinction and absorption cross sections with variation of the interparticle separation distance, when the latter is of the order of the wavelength. We have extended our study to an inhomogeneous complex, consisting of a fixed-size dimer and a monomer at various

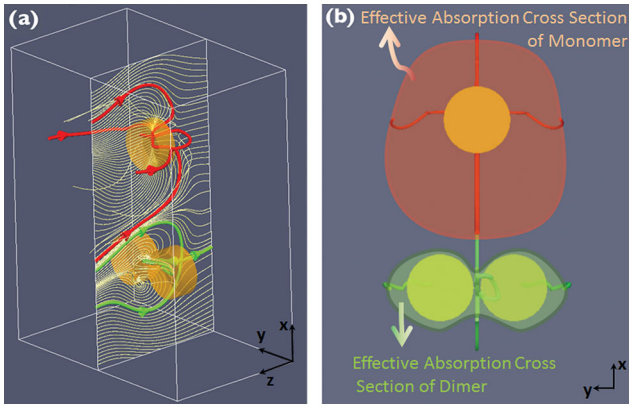

Figure 5. a) 3D view of the Poynting vector field of DpM at wavelength of 571 nm and separation of 365 nm. The boundaries of the vector field lines entering the particles are presented by separatrix tubes. The energy flux inside these tubes is absorbed by the particles. Some characteristic Poynting vector lines on the surface of the separatrix tubes are shown for a monomer by red lines and for a dimer by green ones. b) Geometrical cross sections of the separatrix tubes in the xy-plane, lying in a far field region at $z > 0$, shown as shaded areas for monomer (red) and dimer (green). All lines outside the separatrix tubes do not contribute to the absorption, but contribute to scattering.

distances between them. We showed that at a seperation on the order of the wavelength, both high-energy hybridized mode arising from the dimer and LSPR arising from the monomer get dominated by so called "Young resonance" due to Young's type interference effects. Finally, plots of the Poynting vector fields have revealed two optical vortices situated in front of the dimer, which produce a blockage of the absorption by the dimer, but enhance the scattering by the entire DpM complex; the enhanced absorption at these specific conditions arises because of the ejection of the Poynting vector field by the dimer toward the monomer and the consequent increase in the energy flux for the monomer. Thus, employment of the wavelength-scale interference effects in plasmonic nanosystems may broaden the parameter space for the tuning of the absorption and scattering processes in such systems.

6. Experimental Section

Arrays of Au nanostructures were fabricated on the quartz substrate by electron beam lithography (Elonix 100KV EBL system). Each array has a dimension of $150 \times 150\ \mu m^2$ and a pitch of 2.5 μm in both the x and y directions to avoid coupling among neighboring unit cells. Three nanometer thick Ti film was deposited on the substrate by e-beam evaporation (EB03 BOC Edwards) to increase the adhesion between Au and quartz, followed by an evaporation of 60 nm Au film and a spin-coating of 50 nm hydrogen silsesquioxane (HSQ) as a negative electro-resist. After baking the sample at 200 °C for 2 min, a combined process of e-beam exposure, chemical development, and ion-milling was performed to create well-defined Au nanodisks with diameters of 145 nm and designed configurations on the substrate. Surface morphology of fabricated structures was characterized by a JEOL 7401F Field Emission Scanning Electron Microscope. Spectroscopic characterizations of the fabricated nanoparticle arrays were carried out with a Bruker Hyperion 2000 Fourier transform infrared (FTIR) microscope installed with a 36×, NA = 0.5 objective. The transmission (T) spectrum of each nanoparticle array was obtained by normalizing the transmittance curve from an array-encapsulated area with a reference spectrum taken from a bare area in close proximity to the array. Finally, the extinction spectrum for each array was defined as (1-T).

Three-dimensional (3D) simulations of individual nanostructures were performed by using the finite-difference-time-domain method. In order to calculate extinction cross sections of the studied nanoparticles, we used Lumerical FDTD code to calculate their scattering and absorption plots and the extinction was defined as the sum of scattering and absorption. The substrate effect was fully taken into account in our simulations. CST microwave Studio was employed to map the energy Poynting vectors. In all simulations, the experimental data of Johnson and Christy were used as the dielectric function for gold.[60]

Supporting Information

Supporting Information is available from the Wiley Online Library or from the author.

Acknowledgements

*The authors acknowledge funding provided by SERC Agency of Science, Technology and Research (A*STAR) Superlens Program (Project No. 092 154 0099), the Australian Research Council, and the EPSRC Active Plasmonics Programme as well as the Leverhulme Trust. D. Y. L. acknowledges the grants 1-ZVAL and 1-ZVAW administrated by The Hong Kong Polytechnic University. M. I. T. acknowledges the support from the Russian Fund for Basic Research (Grant No 12–02–00391).*

[1] T. Young, *Philos. Trans. R. Soc. London* **1804**, *94*, 1–16.
[2] D. Smith, J. Pendry, M. Wiltshire, *Science* **2004**, *305*, 788–792.
[3] C. M. Soukoulis, *Science* **2007**, *1136481*, 315.
[4] V. M. Shalaev, *Nat. Photonics* **2007**, *1*, 41–48.
[5] H. Aouani, H. Šípová, M. Rahmani, M. Navarro-Cia, K. Hegnerová, J. Homola, M. Hong, S. A. Maier, *ACS Nano* **2012**, *7*, 669–675.
[6] P. Mühlschlegel, H.-J. Eisler, O. Martin, B. Hecht, D. Pohl, *Science* **2005**, *308*, 1607–1609.
[7] B. Auguié, W. L. Barnes, *Phys. Rev. Lett.* **2008**, *101*, 143902.
[8] B. Lamprecht, G. Schider, R. Lechner, H. Ditlbacher, J. Krenn, A. Leitner, F. Aussenegg, *Phys. Rev. Lett.* **2000**, *84*, 4721–4724.
[9] D. Y. Lei, J. Li, A. I. Fernández-Domínguez, H. C. Ong, S. A. Maier, *ACS Nano* **2009**, *4*, 432–438.
[10] A. Christ, T. Zentgraf, J. Kuhl, S. Tikhodeev, N. Gippius, H. Giessen, *Phys. Rev. B* **2004**, *70*, 125113.
[11] A. O. Pinchuk, G. C. Schatz, *Mater. Sci. Eng. B* **2008**, *149*, 251–258.
[12] K. Li, M. I. Stockman, D. J. Bergman, *Phys. Rev. Lett.* **2003**, *91*, 227402.
[13] K. Li, M. I. Stockman, D. J. Bergman, *Phys. Rev. B* **2005**, *72*, 153401.
[14] A. Bouhelier, R. Bachelot, J. S. Im, G. P. Wiederrecht, G. Lerondel, S. Kostcheev, P. Royer, *J. Phys. Chem. B* **2005**, *109*, 3195–3198.
[15] E. M. Hicks, S. Zou, G. C. Schatz, K. G. Spears, R. P. Van Duyne, L. Gunnarsson, T. Rindzevicius, B. Kasemo, M. Käll, *Nano Lett.* **2005**, *5*, 1065–1070.
[16] E. Yablonovitch, *Phys. Rev. Lett.* **1987**, *58*, 2059–2062.
[17] S. John, *Phys. Rev. Lett.* **1987**, *58*, 2486–2489.
[18] V. Kravets, F. Schedin, A. Grigorenko, *Phys. Rev. Lett.* **2008**, *101*, 087403.
[19] A. Bitzer, J. Wallauer, H. Merbold, H. Helm, T. Feurer, M. Walther, *Opt. Exp.* **2009**, *17*, 22108–22113.
[20] B. Ng, S. Hanham, V. Giannini, Z. Chen, M. Tang, Y. Liew, N. Klein, M. Hong, S. Maier, *Opt. Exp.* **2011**, *19*, 14653–14661.
[21] R. W. Wood, *Proc. Phys. Soc. London* **1901**, *18*, 269–275.
[22] H. F. Talbot, *Philos. Mag. Series 3* **1836**, *9*, 401–407.
[23] B. S. Luk'yanchuk, A. E. Miroshnichenko, M. I. Tribelsky, Y. S. Kivshar, A. R. Khokhlov, *New J. Phys.* **2012**, *14*, 093022.
[24] M. D. Kelzenberg, S. W. Boettcher, J. A. Petykiewicz, D. B. Turner-Evans, M. C. Putnam, E. L. Warren, J. M. Spurgeon, R. M. Briggs, N. S. Lewis, H. A. Atwater, *Nat. Mater.* **2010**, *9*, 239–244.
[25] H. A. Atwater, A. Polman, *Nat. Mater.* **2010**, *9*, 205–213.
[26] J. Hao, J. Wang, X. Liu, W. J. Padilla, L. Zhou, M. Qiu, *Appl. Phys. Lett.* **2010**, *96*, 251104.
[27] C. Wadell, T. J. Antosiewicz, C. Langhammer, *Nano Lett.* **2012**, *12*, 4784–4790.
[28] A. Moreau, C. Ciracì, J. J. Mock, R. T. Hill, Q. Wang, B. J. Wiley, A. Chilkoti, D. R. Smith, *Nature* **2012**, *492*, 86–89.
[29] S. Nie, S. R. Emory, *Science* **1997**, *275*, 1102–1106.
[30] E. Prodan, C. Radloff, N. Halas, P. Nordlander, *Science* **2003**, *302*, 419–422.

[31] N. J. Halas, S. Lal, W.-S. Chang, S. Link, P. Nordlander, *Chem. Rev.* **2011**, *111*, 3913.
[32] P. K. Jain, W. Huang, M. A. El-Sayed, *Nano Lett.* **2007**, *7*, 2080–2088.
[33] V. Giannini, A. I. FernáNdez-DomíNguez, S. C. Heck, S. A. Maier, *Chem. Rev.* **2011**, *111*, 3888.
[34] W. Rechberger, A. Hohenau, A. Leitner, J. Krenn, B. Lamprecht, F. Aussenegg, *Opt. Commun.* **2003**, *220*, 137–141.
[35] L. Gunnarsson, T. Rindzevicius, J. Prikulis, B. Kasemo, M. Käll, S. Zou, G. C. Schatz, *J. Phys. Chem. B* **2005**, *109*, 1079–1087.
[36] C. Dahmen, B. Schmidt, G. Von Plessen, *Nano Lett.* **2007**, *7*, 318–322.
[37] P. Olk, J. Renger, M. T. Wenzel, L. M. Eng, *Nano Lett.* **2008**, *8*, 1174–1178.
[38] H. Fischer, O. J. Martin, *Opt. Lett.* **2009**, *34*, 368–370.
[39] R. Taubert, R. Ameling, T. Weiss, A. Christ, H. Giessen, *Nano Lett.* **2011**, *11*, 4421–4424.
[40] R. Taubert, D. Dregely, T. Stroucken, A. Christ, H. Giessen, *Nat. Commun.* **2012**, *3*, 691.
[41] J. P. Kottmann, O. J. Martin, *Opt. Lett.* **2001**, *26*, 1096–1098.
[42] D. Weber, P. Albella, P. Alonso-González, F. Neubrech, H. Gui, T. Nagao, R. Hillenbrand, J. Aizpurua, A. Pucci, *Opt. Exp.* **2011**, *19*, 15047–15061.
[43] Q. Xu, J. Bao, F. Capasso, G. M. Whitesides, *Angew. Chem.* **2006**, *118*, 3713–3717.
[44] R. Adato, A. A. Yanik, C.-H. Wu, G. Shvets, H. Altug, *Opt. Exp.* **2010**, *18*, 4526–4537.
[45] M. R. Dennis, K. O'holleran, M. J. Padgett, *Prog. Opt.* **2009**, *53*, 293–363.
[46] B. S. Luk'yanchuk, A. E. Miroshnichenko, Y. S. Kivshar, *J. Opt.* **2013**, *15*, 073001.
[47] V. Twersky, *J. Opt. Soc. Am.* **1962**, *52*, 145–169.
[48] V. Twersky, *J. Math. Phys.* **1967**, *8*, 589.
[49] L. Novotny, B. Hecht, *Principles of nano-optics*, 2nd ed., Cambridge University Press, UK **2012**.
[50] M. Hentschel, M. Saliba, R. Vogelgesang, H. Giessen, A. P. Alivisatos, N. Liu, *Nano Lett.* **2010**, *10*, 2721–2726.
[51] K. A. Fuller, *Appl. Opt.* **1991**, *30*, 4716–4731.
[52] P. Albella, M. A. Poyli, M. Schmidt, S. A. Maier, F. Moreno, J. J. Saenz, J. Aizpurua, *J. Phys. Chem. C* **2013**, *117*, 13573–13584.
[53] A. Hemmerich, T. Hänsch, *Phys. Rev. Lett.* **1992**, *68*, 1492–1495.
[54] S. Albaladejo, M. I. Marqués, F. Scheffold, J. J. SáEnz, *Nano Lett.* **2009**, *9*, 3527–3531.
[55] Craig F. Bohren, *Am. J. Phys.* **1983**, *51*, 323.
[56] Z. Wang, B. Luk'yanchuk, M. Hong, Y. Lin, T. Chong, *Phys. Rev. B* **2004**, *70*, 035418.
[57] M. I. Tribelsky, B. S. Luk'yanchuk, *Phys. Rev. Lett.* **2006**, *97*, 263902.
[58] M. I. Tribelsky, *EPL* **2011**, *94*, 14004.
[59] M. Rahmani, B. Luk'yanchuk, M. Hong, *Laser Photon. Rev.* **2012**, *7*, 329–349.
[60] P. B. Johnson, R. Christy, *Phys. Rev. B* **1972**, *6*, 4370.

Received: May 8, 2013
Revised: June 25, 2013
Published online: September 3, 2013

